Available online at www.sciencedirect.com
ScienceDirect
International Journal of Multiphase Flow 34 (2008) 111–127
International Journal of Multiphase Flow
www.elsevier.com/locate/ijmulflow

Experimental study on axial development of liquid film in vertical upward annular two-phase flow

Tatsuya Hazuku [a,*], Tomoji Takamasa [a], Yoichiro Matsumoto [b]

[a] Faculty of Marine Technology, Tokyo University of Marine Science and Technology, Etchujima, Koto, Tokyo 135-8533, Japan
[b] Department of Mechanical Engineering, The University of Tokyo, Hongo, Bunkyo, Tokyo 113-8656, Japan

Received 1 June 2005; received in revised form 9 August 2007

Abstract

Accurate measurements of the interfacial wave structure of upward annular two-phase flow in a vertical pipe were performed using a laser focus displacement meter (LFD). The purpose of this study was to clarify the effectiveness of the LFD for obtaining detailed information on the interfacial displacement of a liquid film in annular two-phase flow and to investigate the effect of axial distance from the air–water inlet on the phenomena. Adiabatic upward annular air–water flow experiments were conducted using a 3 m long, 11 mm ID pipe. Measurements of interfacial waves were conducted at 21 axial locations, spaced 110 mm apart in the pipe. The axial distances from the inlet (z) normalized by the pipe diameter (D) varied over $z/D = 50$–250. Data were collected for predetermined gas and liquid flow conditions and for Reynolds numbers ranging from $Re_G = 31{,}800$ to 98,300 for the gas phase and $Re_L = 1050$ to 9430 for the liquid phase. Using the LFD, we obtained such local properties as the minimum thickness, maximum thickness, and passing frequency of the waves. The maximum film thickness and passing frequency of disturbance waves decreased gradually, with some oscillations, as flow developed. The flow development, i.e., decreasing film thickness and passing frequency, persisted until the end of the pipe, which means that the flow might never reach the fully developed state. The minimum film thickness decreased with flow development and with increasing gas flow rate. These results are discussed, taking into account the buffer layer calculated from Karman's three-layer model. A correlation is proposed between the minimum film thickness obtained in relation to the interfacial shear stress and the Reynolds number of the liquid.
© 2007 Elsevier Ltd. All rights reserved.

Keywords: Flow measurement; Laser focus displacement meter; Interfacial wave; Film thickness; Axial development; Annular two-phase flow

1. Introduction

Annular two-phase flow is the most common flow pattern in boiling heat transfer systems, such as the boilers and heat exchangers in many energy plants. The flow characteristics of liquid films in annular two-phase flow, especially the wave phenomena on a liquid film, play important roles in heat and mass transfer. The

* Corresponding author. Tel.: +81 3 5245 7727; fax: +81 3 5245 7410.
E-mail address: hazuku@kaiyodai.ac.jp (T. Hazuku).

0301-9322/$ - see front matter © 2007 Elsevier Ltd. All rights reserved.
doi:10.1016/j.ijmultiphaseflow.2007.10.008

phenomena are closely related to the process of transition to liquid film dryout, which can lead to fatal problems for plant safety and efficient operation. Accurate knowledge of the interfacial structure of liquid films in annular flow is thus essential for proper thermal-hydraulic design and safety analysis of plants.

The interfacial structure of a liquid film in annular flow changes continuously with flow development in the axial direction, because the axial pressure changes and the interfacial shear stresses are very large compared with those of other flow patterns. Therefore, detailed axial measurements of the local flow parameters of liquid films are required for the successful development of theoretical models of annular two-phase flow systems. While a majority of two-phase flow characteristics can now be predicted numerically due to recent advances in numerical simulation techniques, reliable experimental data concerning the time dependency and instantaneous local characteristics of two-phase flow structures are required to confirm the validity of these simulations. Thus for the study of annular two-phase flow it has been necessary to develop a measuring technique to obtain detailed liquid film information with high spatiotemporal resolution and no disturbance of the flow.

In past studies of quantitative features of thin flowing liquid films in pipes, some researchers have used visualization techniques such as shadowgraphs (Ohba et al., 1995; Clark et al., 1999) or laser-induced fluorescence (Hewitt et al., 1985). These techniques are limited by reflection and refraction of the laser sheet passing through the fluid and a transparent pipe wall, which reduces their spatial measurement accuracy, especially at the smallest scale. With electrical methods, film thickness can be calculated from the resistance or capacitance of the fluid between sensors. These techniques are useful for measuring spatial average values of a continuous film (Poltalski and Clegg, 1972; Mori et al., 1998; Elsäßer et al., 1998; Dukler and Bergelin, 1952; Hewitt and Hall-Taylor, 1970). However, instantaneous film thickness cannot be measured, especially for very thin films or at the level of fine detail required to record the structure of superimposed waves. Some researchers have used a laser displacement gauge (Serizawa et al., 1994; Nasr-Esfahany and Kawaji, 1996) and supersonic echo methods (Serizawa et al., 1995) to measure film thickness. The laser displacement gauge, composed of a semiconductor laser and a position-sensitive detector, detects the target position using a triangular relationship. In this method, the laser beam is reflected from the target and onto a position-sensitive detector. In the supersonic echo method, film thickness can be detected from the delay of the signal reflected from the liquid surface. These techniques provide high spatial resolution and do not disturb the flow. However, they also present two problems: (1) they cannot detect a very thin film because the reflected signal from the wall surface interferes with that from the film surface, and (2) if the curvature of the interfacial wave is large, the reflected beam or sonic wave cannot reach the detector. Displacements of very thin films, as well as small waves or waves with large surface curvature, cannot be measured accurately with these techniques.

Recently, a new laser focus displacement meter (LFD, Keyence Co., Japan, Model LT 8100) was developed to detect scratches on ICs and other electronic devices. This sensor has the potential to solve the curvature problem and to measure waves on films at high spatial and temporal resolutions, even on thin films. In previous experiments conducted by Takamasa and Hazuku (2000) and Takamasa and Kobayashi (2000), interfacial waves on a film flowing down a vertical plate wall and down the inner wall of a pipe were measured using an LFD. The effectiveness of the new method for obtaining detailed liquid film information was clarified in these studies.

As previously mentioned, precise spatiotemporal knowledge of the interface in annular two-phase flows is essential to understanding the details of the fascinating nonlinear phenomena of the interface in a channel. In this study, we measured the microscopic interfacial wave structure of vertical annular two-phase flow using the LFD method. The purpose of the study was to clarify the effectiveness of the LFD for obtaining detailed information concerning the interfacial displacement of a liquid film in annular two-phase flow and to investigate the behavior of the flow development of liquid films in the axial direction. Adiabatic upward annular two-phase flow experiments were conducted using a 3 m long, 11 mm ID pipe, and measurements of local film thickness were taken at 21 axial locations. Although considerable effort has been expended in the past to study the behavior of liquid films in a fully developed region (2–4 m below the inlet), very few detailed measurements have been made of the phenomena in a developing flow, which is considered more important for industrial design and useful for the improvement of existing analytical models and for finding empirical correlations to aid in predicting flows.

2. Measurement accuracy of liquid film thickness

Fig. 1 shows a schematic diagram of the LFD. The displacement of the target can be determined by registering the displacement of an objective lens that is continuously moved at a known frequency by a tuning fork, when the laser beam passing through the objective lens is focused on the target (Takamasa and Hazuku, 2000). The principle behind the LFD measurement of the distance between the sensor and target is the same as that of a camera focusing on a target with a motor-driven objective lens in daylight. This principle makes accurate measurement of the wave height or film thickness possible, even if the wave surface has a large curvature. The sensor has a measurement range of 28 ± 1 mm from the laser head. The diameter of the beam spot is 2 μm, and the spatial resolution is 0.2 μm. The temporal resolution is approximately 1 kHz.

It is possible to measure a liquid film on the inner wall of a transparent pipe using the LFD from outside the pipe. However, it is necessary to estimate the displacement error introduced by refraction of the laser beam passing through both surfaces of the pipe. When the conical laser beam from the LFD reaches the target of the film surface, the beam scatters and is reflected from the target back into the LFD. However, no clean point focus is possible, because the beam cone must traverse the wall of the pipe, which forms a cylindrical lens. The consequent widening and scattering reduce the brightness of the reflected beam below the detection threshold of the light sensor. Therefore, it is difficult for the LFD to measure the thickness of a liquid film on a pipe inner wall when the usual tubular geometry is used. In the previous study (Takamasa and Kobayashi, 2000), a preliminary test was conducted to identify an appropriate measuring method that would solve this problem. The preliminary test showed that the brightness of light reflected from the surface of the film on the pipe's inner wall was high enough to be detected by the light sensor when the wall's outer surface was flat. The displacement error caused by refraction of the laser beam passing through an acrylic pipe with a flat outer wall surface and through water was also estimated. When acrylic and pure water are used respectively as the pipe material and the working fluid for the liquid phase, the theoretical equation for correction of the refraction error is expressed by the following equation:

$$\delta = \left[1.33 + 0.356\frac{\delta_M}{D}\right]\delta_M, \tag{1}$$

where D is the pipe inner diameter and δ_M is the measured film thickness. When the film thickness is calculated from the displacement difference between the fluid and window surface, the equation shows that the corrected

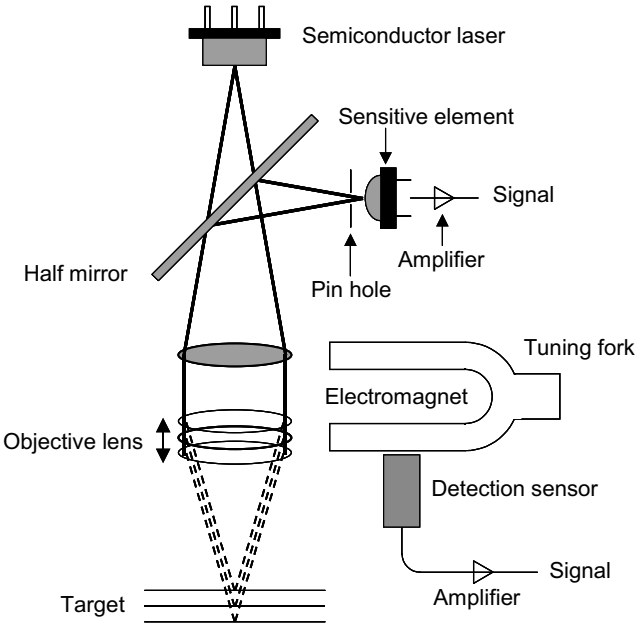

Fig. 1. Principle of laser focus displacement meter.

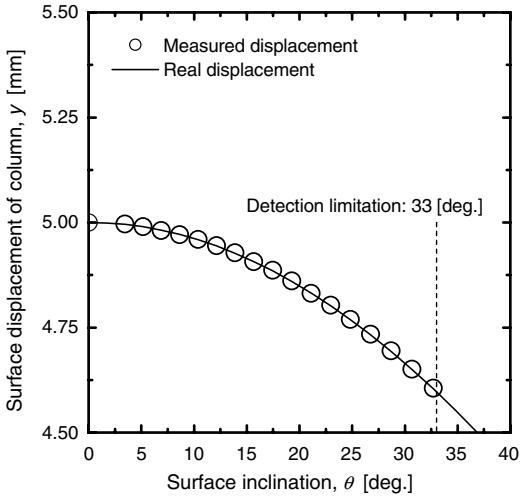

Fig. 2. Measuring limitation due to surface inclination.

film thickness, δ, is independent of the thickness of the window and the distance from the laser head to the window. The displacement error found with this preliminary test showed that the film thickness calculated with Eq. (1) agrees with the true film thickness to within 1%. This equation is useful when $D = 10$–30 mm and $\delta <= 2.4$ mm.

As mentioned previously, the LFD can measure surface displacement even if the curvature or inclination angle of the surface is large. Although inclination problems affecting the detection limits of the LFD are insignificant compared with those of conventional film measurement techniques, the LFD's measurement capabilities for film thickness must be checked. A preliminary test of this was carried out in this study, using a glass column 5 mm in diameter. In the test, the LFD measured the vertical displacement of the column surface. Fig. 2 shows the measured surface displacement versus surface inclination. Open circles and the solid line represent measured and real displacements calculated from the horizontal location of the target. As shown in the figure, detection was incomplete when the angle of surface inclination was larger than 33°. The detection limit of the surface inclination angle versus the axis of the conical beam is expected to be 33°.

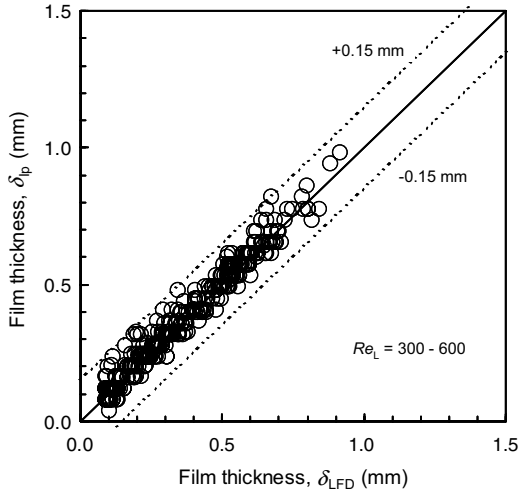

Fig. 3. Error estimates for film thickness as measured by LFD and by image processing.

A second preliminary test was performed to compare the interfacial displacement of a liquid film as measured by LFD with that obtained by image analysis using a high-speed video camera. The falling liquid film formed in a vertical rectangular pipe 3 mm wide was measured in the test. Interfacial conditions of the liquid film were varied by the introduction of nitrogen gas. The LFD detected transient changes of interfacial waves very well, even when the surface elevation and inclination of the film changed rapidly, and could measure the bottom point of the interfacial wave or the local minimum film thickness, which had never been measured accurately with conventional measuring techniques.

Fig. 3 shows the result of error estimation of film thickness measured by LFD and image analysis. The methods agree well, within 0.15 mm, although they include errors caused by low spatial resolution in the images and distortion of the image due to capillarity near the wall surface.

3. Apparatus for annular two-phase flow experiment

Fig. 4 shows the two-phase flow loop used in the present experiments. The working fluids were air and pure water, which was obtained by purifying tap water to an electrical conductivity lower than 1 μS/cm. Air was fed into the channel from a compressor. The water was pumped from a water tank into a test pipe made of acrylic, passed through a flow meter, and piped back to the water tank. A uniform liquid film was generated by a sintered metal pipe. The inside diameter and length of the test pipe were 11 mm and 3 m, respectively. Water

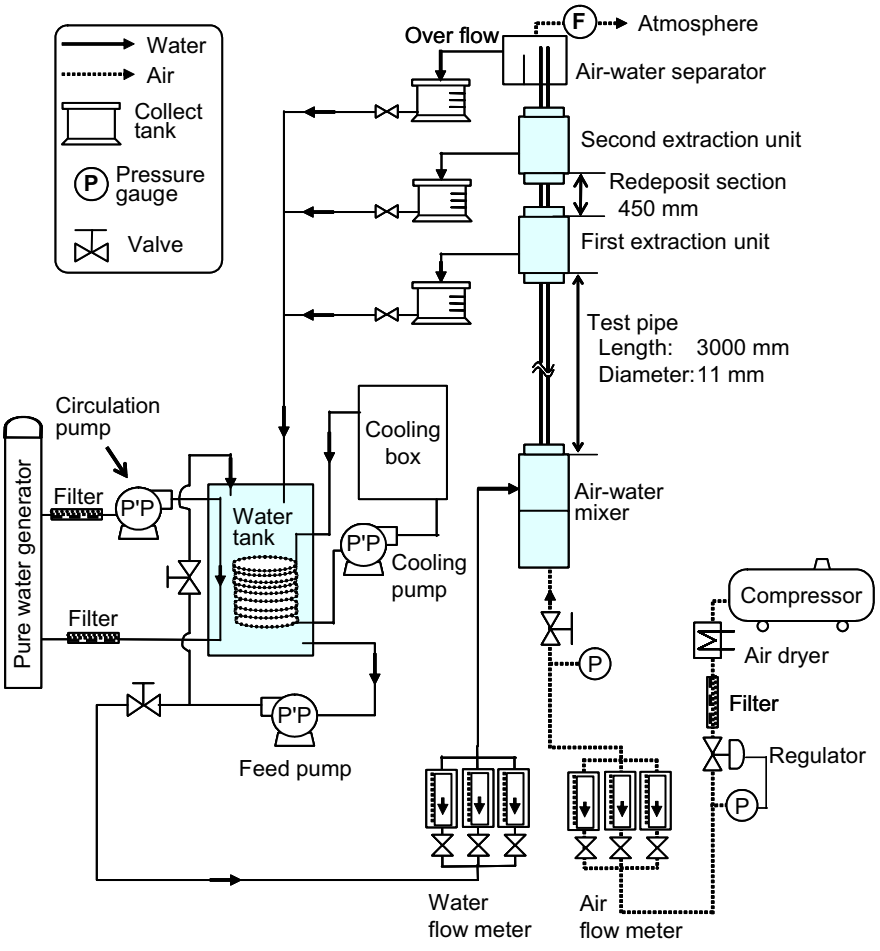

Fig. 4. Annular two-phase flow loop.

temperature was maintained at 25 ± 0.5 °C by a cooler submerged in the water tank. Thermocouples in the water tank and separation tank monitored the water temperature. Measurements of film thickness were conducted at 21 axial locations, equally spaced 110 mm apart along the length of the pipe. The axial distance from the inlet (z), normalized by the pipe diameter (D), was $z/D = 50$–250. Data were collected for predetermined gas and liquid flow conditions and for Reynolds numbers ranging from $Re_G = 31{,}800$ to 98,300 for the gas phase and $Re_L = 1050$ to 9430 for the liquid phase. The displacement of the gas–liquid interface in the test channel was measured using the LFD. The phenomena were recorded by a high-speed video camera operating at 1000 frames per second and synchronized with the film thickness measurement. A trigger signal started both the LFD and the camera.

4. Results and discussion

4.1. Axial variation of liquid film flow

Fig. 5 shows typical film thickness traces obtained at distances of 550, 1650, and 2750 mm from the water inlet. As shown in this figure, the wave on the interface consisted of ripples smaller than 0.1 mm and disturbance waves with large amplitude and high velocity. Although conventional electrical methods, such as electrical–resistance and electrical–capacitance techniques, cannot measure such fine waves because these techniques obtain the liquid film thickness as a spatially averaged value in the area between the electrodes (approximately 5 mm), the LFD method can detect and record the details very well. Film thickness and wave amplitude decreased with distance from the entry. This occurs because the gas velocity and the interfacial shear stress increase as flow develops due to the pressure gradient in the axial direction. Fig. 6 shows the effect of entry length on the interfacial shear stress under various flow conditions. The interfacial shear stress, τ_i, was calculated with the following equation:

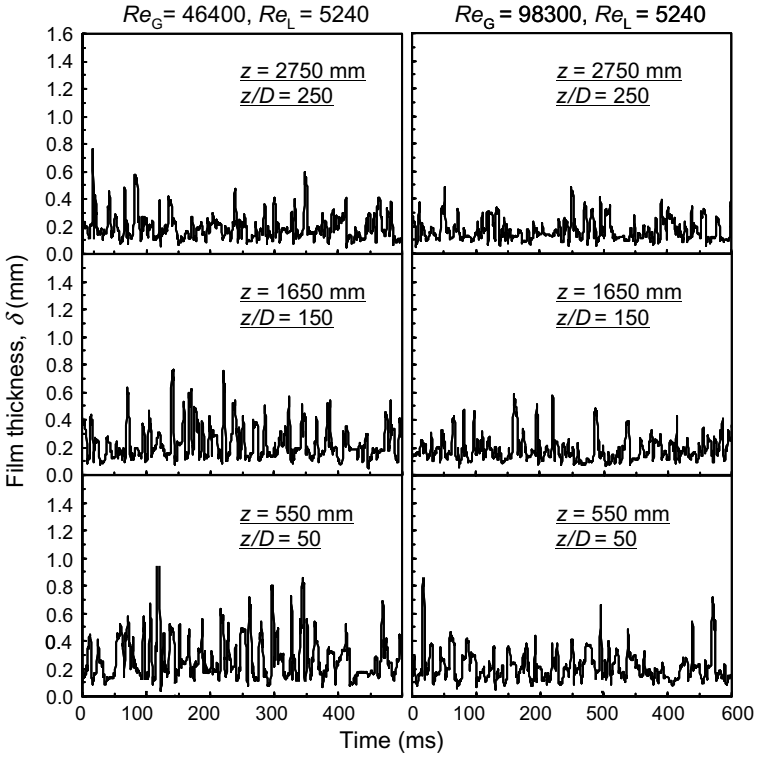

Fig. 5. Typical film thickness traces in annular flow.

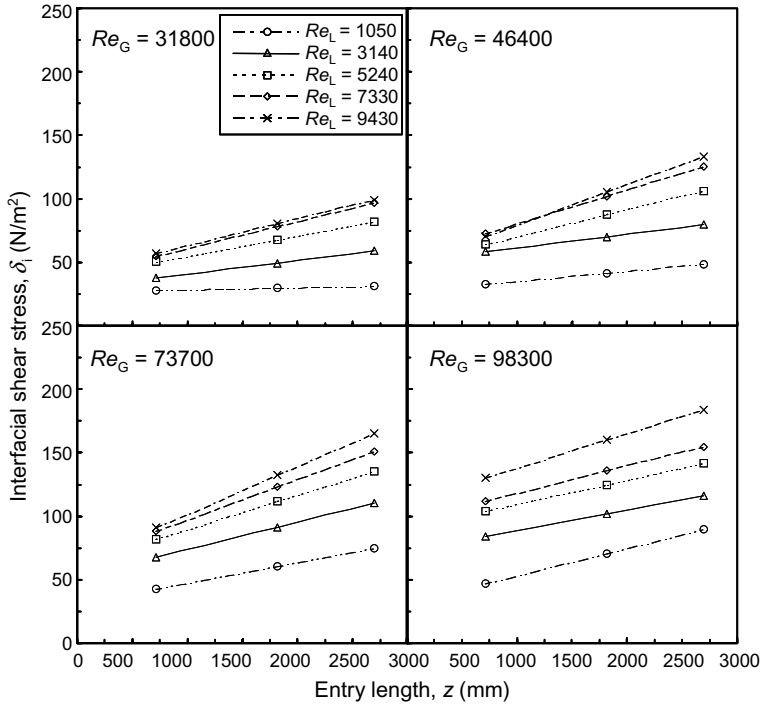

Fig. 6. Interfacial shear stress.

$$\tau_i = \frac{D_i}{4}\left(\frac{dp_G}{dz}\right)_F, \quad D_i = D - 2\bar{\delta}, \tag{2}$$

where D and $\bar{\delta}$ represent the pipe diameter and the time-averaged film thickness, respectively. The pressure gradient due to friction loss, $(dp_G/dz)_F$, was calculated from the differential pressure and the time-averaged film thickness at each axial location. As shown in the figure, the interfacial shear stress increased with entry length under all flow conditions. The liquid film thickness and entrainment from the interface were closely related to the interfacial shear stress. In the past, many two-phase flow film models were proposed based on fully developed flow under hydrodynamic equilibrium. Our experimental results, however, indicate that the fully developed flow assumption is not acceptable for vertical annular two-phase flow under low pressure because frictional pressure change in the axial direction cannot be ignored.

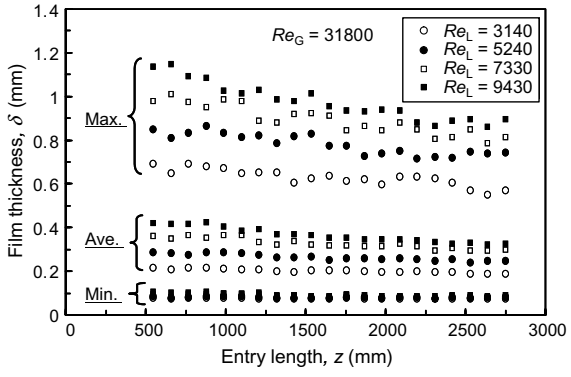

Fig. 7. Axial change of film thickness in annular flow ($Re_G = 31{,}800$).

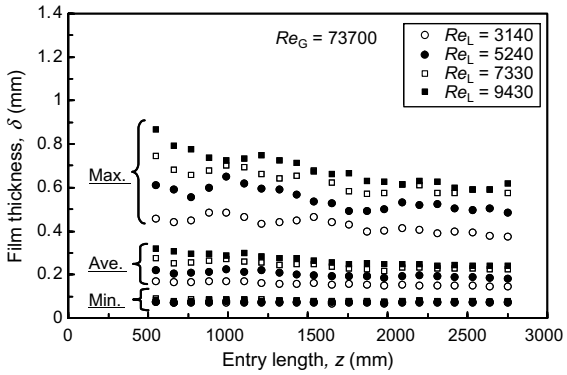

Fig. 8. Axial change of film thickness in annular flow ($Re_G = 73{,}700$).

Figs. 7 and 8 show the changes in maximum, minimum, and average film thickness in the axial direction. The minimum and maximum film thicknesses were calculated to represent the 1% and 99% probability levels, respectively. Maximum film thickness decreased gradually, with some oscillation, as flow developed along the pipe. Changes in the maximum film thickness continued down to the pipe exit. Therefore, flow might not reach the fully developed state. On the other hand, minimum film thickness showed a tendency to decrease slightly with distance from the entry.

We investigated the characteristics of disturbance wave frequency at each axial location, with transient data on film thickness obtained by the LFD. According to the latest report, dry-patch generation is strongly related to behavior of the disturbance wave. Fukano et al. reported the mechanism behind dry-patch generation in a narrow annular channel under atmospheric pressure (Fukano et al., 2002, 2003). They explained the existence of a dry patch in a thin liquid film with two mechanisms. For relatively low vapor velocity, a dry patch occurs because of drainage between long-interval disturbance waves, with a very thin base film. This means that the occurrence of burnout is strongly dependent on the passing frequency of disturbance waves and the behavior of a thin base film, i.e., the local minimum film thickness. Many theoretical and experimental studies have focused on such characteristics of disturbance waves as wave velocity, passing frequency, and wave height (Hall-Taylor and Nedderman, 1968; Hewitt and Nicholls, 1969; Azzopardi, 1986; Sekoguchi and Mori, 1997). The interface on the film consists of waves having components with a wide range of frequencies and amplitudes. Although the classification of these waves has been an interesting topic for a long time, there is no consensus about, or clear definition of, this classification at present. In this study, the interfacial waves on a liquid film were classified as shown in Fig. 9. A disturbance wave is defined as a wave whose thickness at both ends is smaller than the average film thickness, and a wave with a peak greater than the average thickness of upper wave layer, δ_H calculated from the following equation:

$$\delta_H = \frac{1}{n}\sum_{k=1}^{n}\delta_k, \quad (\delta_k > \bar{\delta}). \tag{3}$$

We performed a cross-calibration on the disturbance wave measurements at the frequencies observed with the high-speed video camera and those observed with the LFD. Film thickness traces obtained with the LFD and corresponding flow images are shown in Fig. 10. Open circles in the figure mark the disturbance waves defined by the above criteria. Because the velocity and amplitude of the disturbance waves are much higher and larger than those of other types of waves, disturbance waves can easily be identified in images and traces. As shown in the figure, the disturbance waves passing through the measuring position in the images coincide with those in the LFD measurements. The disturbance wave frequencies obtained by the LFD method agree with those observed in the images to within 15%.

We also compared our data with predictions made by a correlation proposed by Sekoguchi et al. (1985). They measured disturbance waves in 8–26 mm ID pipe with gas superficial velocities ranging from $j_G = 20$ to 50 m/s, liquid superficial velocities ranging from $j_L = 0.04$ to 0.14 m/s, and axial locations from

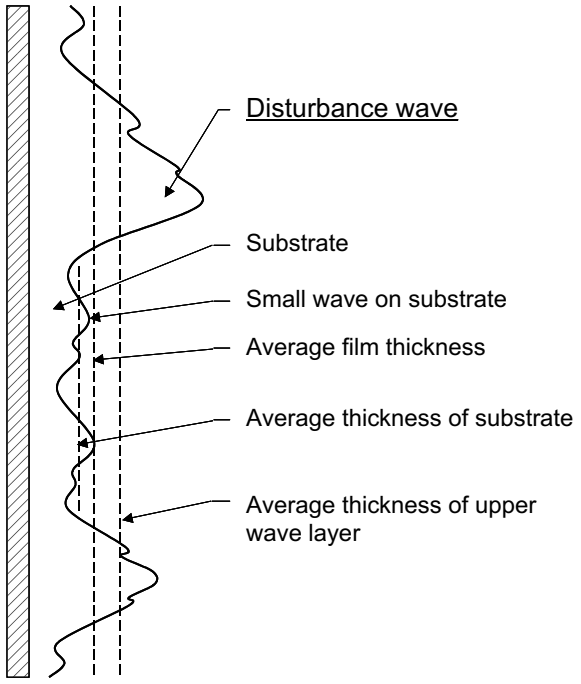

Fig. 9. Classification of interfacial waves on a liquid film.

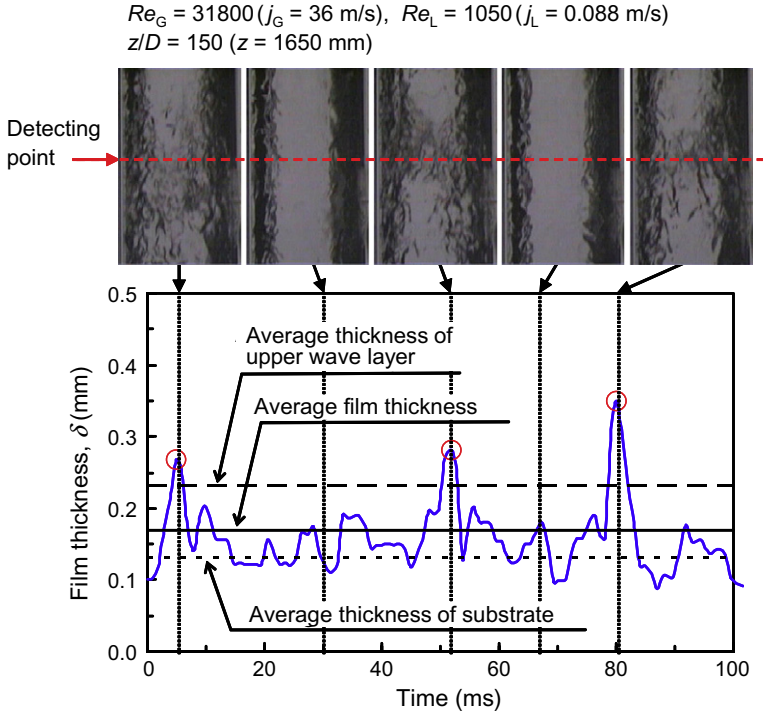

Fig. 10. Video images of disturbance waves and film thickness trace measured by LFD.

$z = 3100$–4200 mm ($z/D = 162$–388). Proposed equation (4) for the disturbance wave frequency, f_D, with Strouhaul number, Sr, and Eötvös number, $Eö$, can predict their experimental results to within $\pm 10\%$ in average relative deviation.

$$
\begin{aligned}
&Sr = f_D \cdot D/j_G = f_1(E\ddot{o}) \cdot g_1(\xi),\\
&f_1(E\ddot{o}) = E\ddot{o}^{-0.5}(0.5\ln E\ddot{o} - 0.47),\\
&g_1(\xi) = 0.0076\ln\xi - 0.051,\\
&E\ddot{o} = gD^2(\rho_L - \rho_G)/\sigma,\\
&\xi = Re_L^{2.5}/Fr_G,\\
&Fr_G = j_G/\sqrt{gD},
\end{aligned}
\tag{4}
$$

where g, ρ_L, ρ_G, σ, and Fr_G are the acceleration of gravity, liquid density, gas density, surface tension, and Froude number of the gas phase, respectively. Fig. 11 shows the comparison between our measured disturbance wave frequencies at $z = 2310$–2750 mm ($z/D = 210$–250) and those predicted by Eq. (4). Although Eq. (4) predicts slightly higher frequencies than our experimental data at high gas flow rates, the two sets agree to within 25%. This result demonstrates the validity of Eq. (4) for an entry region.

Although the above correlation (4) predicts the present disturbance wave frequency closely at some axial distances, the liquid film varies in thickness and wave height along the pipe, as shown in Figs. 7 and 8. We accordingly checked the axial change of disturbance wave frequency. Figs. 12 and 13 show the development of disturbance wave frequency in the axial direction. As shown in the figures, the disturbance wave frequency decreased gradually with some oscillations along the pipe, evidencing the same changes as the results of the maximum film thickness. The results suggest that axial changes of wave frequency should be considered in the modeling of films in annular two-phase flow.

In this study, we examined such interesting phenomena as that the maximum film thickness and the disturbance wave frequency decreased along the pipe, with some oscillations. K in Eq. (5) is the kurtosis, which is the value of the fourth moment of thickness data in a time series, normalized by the quadruplicate standard deviation of the film thickness, ψ^4. It indicates the macroscopic interfacial wave structure such as wave steepness and intensity of wave amplitude.

$$
K = \frac{\sum_{k=1}^{n}(\delta_k - \bar{\delta})^4}{n \cdot \psi^4}, \tag{5}
$$

Fig. 14 shows the effect of axial distance on K. The K has some extreme values in the axial direction depending on liquid flow rate. This means that steady fluctuation of wave velocity and amplitude exists at each axial location. It is possible that a pressure resonance interaction is closely involved in this interesting phenomenon. If formation of a standing pressure wave is induced in the annular-mist flow region, the liquid droplets and

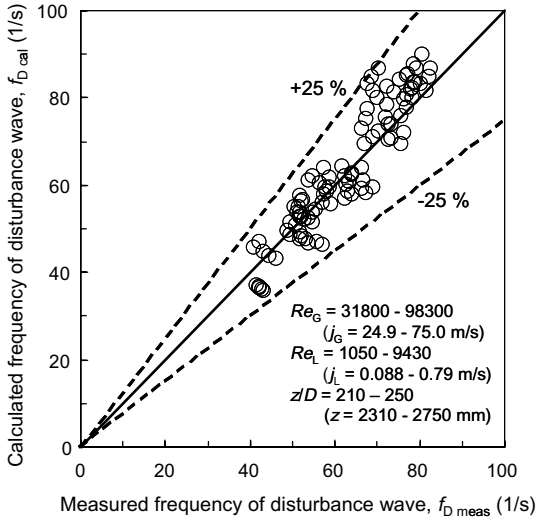

Fig. 11. Comparison between measured disturbance wave frequency and that predicted by Eq. (4).

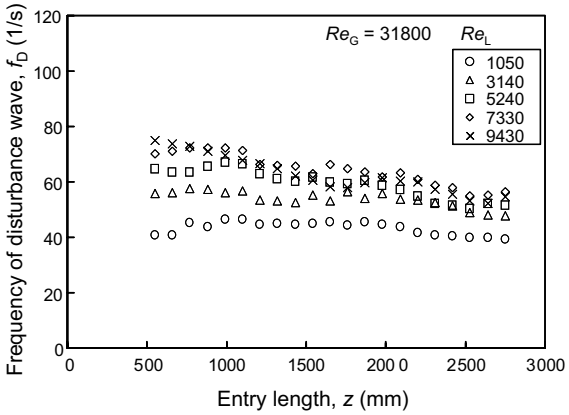

Fig. 12. Frequency of disturbance wave in annular flow ($Re_G = 31{,}800$).

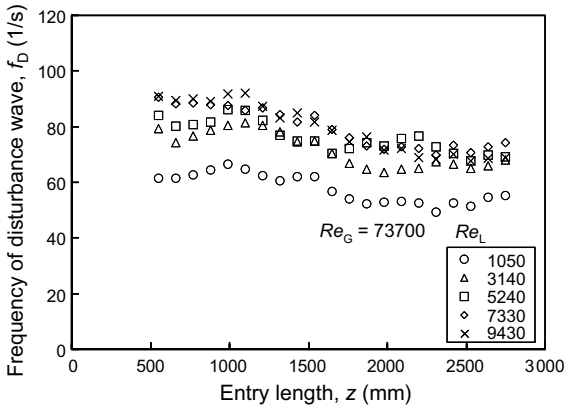

Fig. 13. Frequency of disturbance wave in annular flow ($Re_G = 73{,}700$).

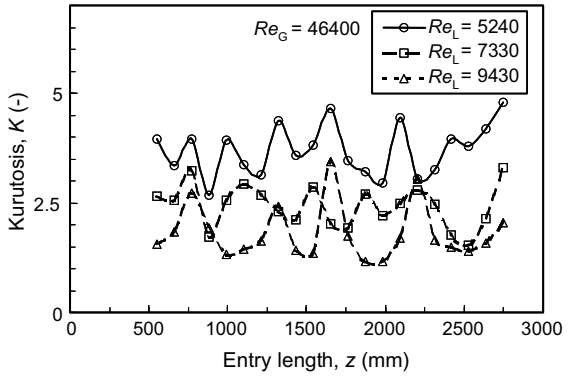

Fig. 14. Interfacial sharpness on liquid film (kurtosis).

waves should be held with regularity along the pipe, depending on the profile of the standing pressure wave, and this may follow from the fact that steady fluctuations of the maximum film thickness and disturbance wave frequency occur at each axial position in the pipe. In view of this, the measurement of pressure wave propagation in the pipe was examined. Phase-delay of pressure wave propagation in the pipe, ω in Fig. 15, was measured by two pressure gauges installed along the pipe. The case of $\omega > 0$ indicates the formation of

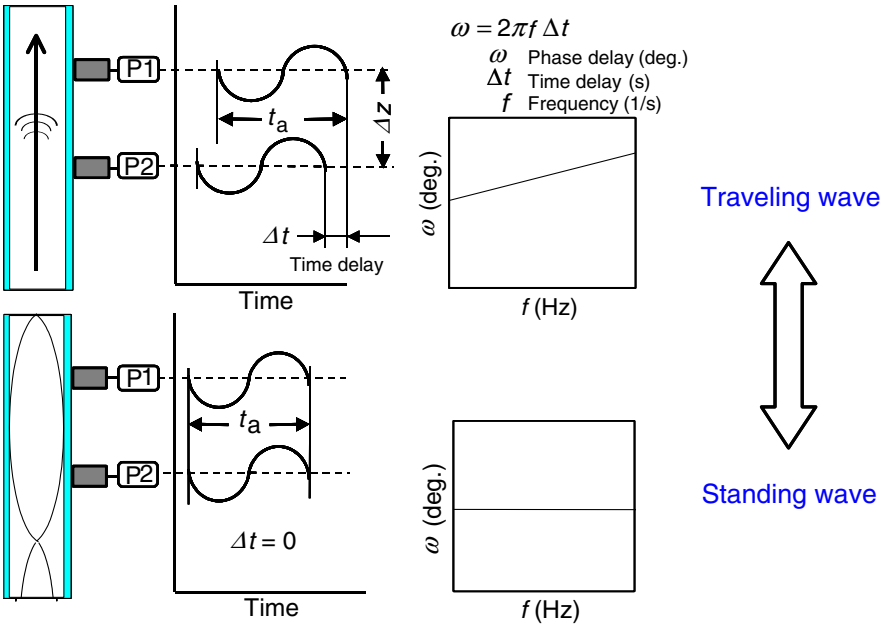

Fig. 15. Traveling and standing waves of pressure in the pipe.

a traveling wave propagating in the axial direction. A standing wave is indicated by $\omega = 0$. Measurements of pressure propagation were carried out at axial locations of $z = 550$, 1650, and 2750 mm, and the distance between the pressure gauges at each location was set at 33 mm.

As shown in Fig. 16, phase delays of pressure propagation varied with increase in axial distance, and formation of standing waves with a frequency of around 50 Hz was confirmed. Although the pressure propaga-

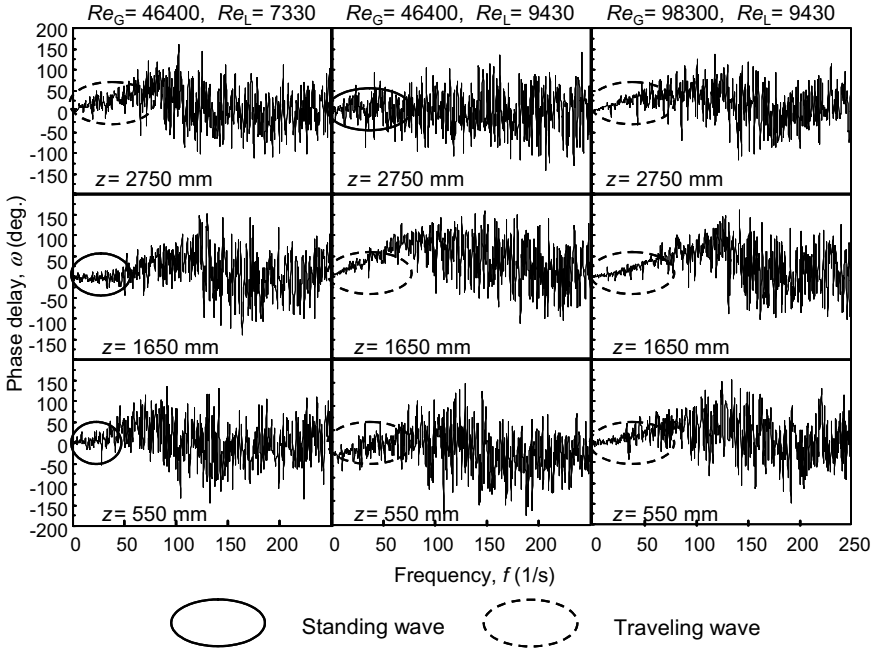

Fig. 16. Phase delay of pressure waves in annular flow.

tions at all axial locations were not measured simultaneously, it is possible that such local characteristics of the pressure propagation at each axial location are involved in producing the steady fluctuation of maximum film thickness and disturbance wave frequency in the axial direction. In a future study, the mechanism behind this phenomenon should be clarified by conducting detailed measurements of pressure profile, film thickness, and wave frequency in the axial direction.

4.2. Minimum film thickness

As mentioned in the previous section, the occurrence of burnout is strongly dependent on the behavior of the thin base film and the passing frequency of disturbance waves. Because of the inherent shortcomings in conventional techniques for film measurement, we had no good database of the microscopic structure of thin films, i.e., the local minimum film thickness. LFD may be the only method that allows high-accuracy spatio-temporal measurement of local minimum film thickness.

Data on minimum film thickness measured by the LFD are introduced and discussed below. Fig. 17 shows the effect of relative Reynolds number of the gas phase, Re_{Gi}, on the dimensionless minimum film thickness, δ^*_{min}, defined by

$$\delta^*_{min} = \delta_{min}(g/\nu_L^2)^{1/3}, \tag{6}$$

$$Re_{Gi} = u_G D_i/\nu_G, \tag{7}$$

where ν_L, ν_G, and u_G represent the kinematic viscosity of liquid, kinematic viscosity of gas, and mean gas velocity, respectively. Crosses in the figure represent the minimum film thicknesses measured by Ueda and Nose (1973), which were obtained with a needle contact technique. It is expected that viscous forces from the wall will have a strong effect on such a thin flowing film. We therefore checked the relationship between the present data and the thickness of the viscous sub-layer. The dimensionless distance from the wall, y^+, is given by

$$y^+ = \frac{y}{\nu_L}\sqrt{\frac{\tau_w}{\rho_L}}. \tag{8}$$

Assuming that the acceleration loss and momentum change due to entrainment are negligible, wall shear stress, τ_w, in Eq. (8) is given by

$$\tau_w = \frac{D}{4}\left(\frac{dp}{dz}\right)_F, \tag{9}$$

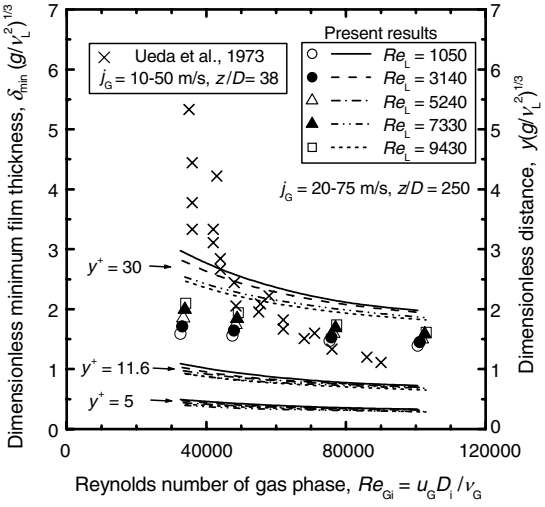

Fig. 17. Minimum film thickness.

where $(dp/dz)_F$, is friction loss calculated by the differential pressure and time-averaged film thickness at each axial location. In the Karman two-layer model, the viscous sub-layer is defined in the range $y^+ \leqq 11.6$. On the other hand, in the three-layer model, the viscous sub-layer is defined in the range $y^+ \leqq 5$, and the buffer layer is defined in the range $5 < y^+ \leqq 30$. Lines in the figure indicate the distance from the wall, $y(g/v_L^2)^{1/3}$, when y^+ is 5, 11, and 30, respectively.

As shown in the figure, although the tendency of the minimum film thickness to decrease with the Reynolds number of the gas phase is consistent, the effect of Reynolds number on the present minimum film thickness is much smaller than that in the results of Ueda et al. The present results also show that the dependence of liquid flow rate is stronger than that of gas flow rate. At low gas flow rates, the results obtained by Ueda et al. are larger than those in the present study. This discrepancy might be attributed to the meniscus problem in the needle contact technique. This technique measures film thickness as greater than the actual value due to the presence of a meniscus at the needle tip, as Ueda et al. pointed out (Ueda and Nose, 1973). Also, the values in their results are smaller than those in our study for high gas flow rates. This discrepancy may be caused by expansion of the acrylic pipe owing to high inside pressure under high gas flow conditions. In other words, the needle contact technique may report a thinner film than the actual value because the distance between needle tip and liquid film surface, which is opposite to the needle, increases owing to an increase in pipe diameter. As for the pipe expansion effect in Ueda's experiments, the internal wall displacements due to the expansion, estimated by a stress analysis based on the tube radius and thickness they used, varied in the range 9–13 μm $[\delta_{min}(g/v_L^2)^{1/3} = 0.2 - 0.3]$. Taking these displacements into account, our results agree well with theirs.

It should be noted here that the interfaces at minimum film thickness in the present experiment extend into the buffer layer in all flow conditions, and the tendency to decrease in thickness with gas flow rate is similar to that of the viscous sub-layer. These results reveal that minimum film thickness is strongly affected by the viscous sub-layer, i.e., viscous forces on the wall. Figs. 18 and 19 show the frequency of the bottom point of the interfacial wave, i.e., the passing frequency of a local minimum point in the buffer layer. The frequency of a bottom point dipping into the buffer layer increases with decreasing liquid flow rate; it extends above 120 Hz in low liquid flow conditions with $Re_L = 1050$. Although the values tend to increase slightly with distance from the entry for a high liquid-to-gas flow ratio ($Re_G = 46{,}400$; $Re_L = 5240$–9430) and short entry length ($z < 2000$ mm) they are effectively constant irrespective of gas flow rate and entry length changes. Considering that these results show that the minimum film thickness and frequency of the bottom point of an interfacial wave in the buffer layer are constant with regard to changes in thickness of the buffer layer, the behavior of local minimum film thickness may be determined by a balancing action between the interfacial shear stress and viscosity force on the wall. We therefore formulated an experimental correlation for predicting the minimum film thickness in gas–liquid upward annular flow. It was confirmed that the minimum film thickness decreases with increasing distance from the entry, gas flow rate, i.e., interfacial shear stress, as well as with decreasing thickness of the viscous sub-layer. As mentioned, the interfacial shear stress is a function of entry length, gas

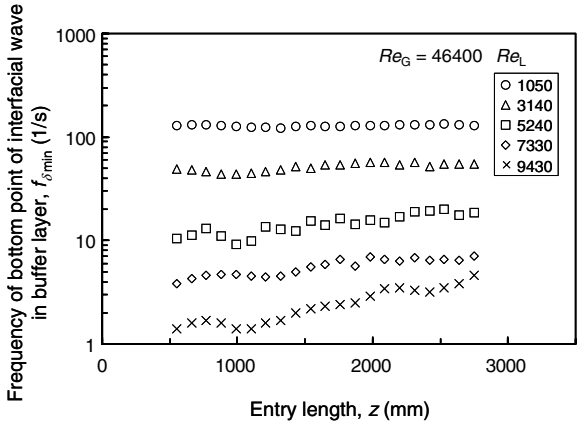

Fig. 18. Frequency of bottom point of interfacial waves in buffer layer ($Re_G = 46{,}400$).

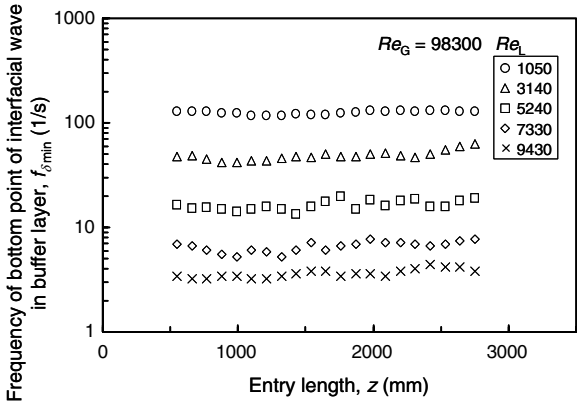

Fig. 19. Frequency of bottom point of interfacial waves in buffer layer ($Re_G = 98{,}300$).

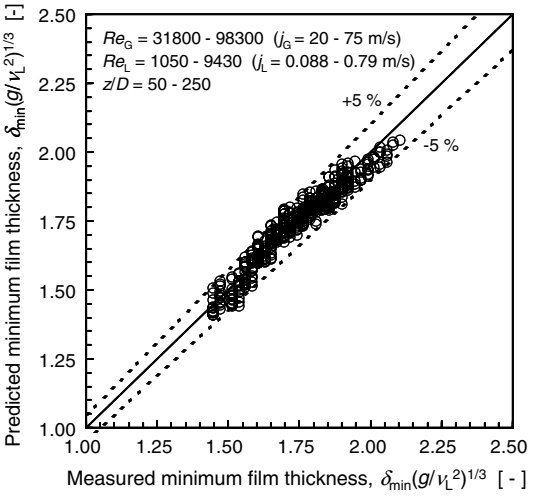

Fig. 20. Comparison between the measured dimensionless minimum film thickness and that predicted by Eq. (10).

flow rate, and thickness of the viscous sub-layer. The following correlation is proposed for minimum film thickness with regard to interfacial shear stress and the Reynolds number of the liquid:

$$\delta^*_{\min} = 0.977 Re_L^{0.143} \tau_i^{*-0.117}, \quad \tau_i^* = \frac{\tau_i}{\rho_L g}\left(\frac{g}{\nu_L^2}\right)^{1/3}$$
$$(Re_G = 31,800\text{–}98,300, \quad Re_L = 1050\text{–}9430, \quad z/D = 50\text{–}250). \tag{10}$$

Fig. 20 shows the comparison between the minimum film thickness predicted by Eq. (10) and that measured with the LFD. As shown in the figure, the present data are accurately described by the experimental Eq. (10) to within 5%. The effect of pipe diameter and other geometric properties, which are not accounted for in Eq. (9), should be further investigated in future studies.

5. Conclusions

This report presents an experimental study of interfacial waves on liquid films in an upward annular air–water two-phase flow using a laser focus displacement meter (LFD). The purpose of this study was to clarify the effectiveness of the LFD for obtaining detailed information concerning the interfacial displacement of a

liquid film in annular two-phase flow and to investigate the effects of axial distance from the air–water inlet. We conducted a preliminary test with simultaneous measurements of the liquid film interface in an acrylic rectangular pipe 3 mm wide, using LFD and high-speed video camera to check the measuring accuracy of the LFD. Using the LFD, we obtained a precise database of such interfacial wave characteristics as the minimum thickness, maximum thickness, and passing frequency of the waves, with regard to flow development along a 3 m long, 11 mm ID pipe. The results are summarized as follows:

A preliminary test showed that the LFD could record transient changes in interfacial waves very well even when the surface elevation and inclination changed rapidly, and could measure the bottom point of an interfacial wave or the local minimum film thickness, which has never been measured accurately with conventional measuring techniques.

The maximum film thickness and passing frequency of disturbance waves decreased gradually, with some oscillations, as flow developed. The flow development, i.e., decreases of film thickness and passing frequency, persisted until the pipe exit, which means that the flow might never reach a fully developed state. These phenomena were also discussed from the viewpoint of pressure resonance interactions based on the experimental measurement of pressure propagation in the pipe. The minimum thickness of the film decreased with flow development and with increasing gas flow rate. These results were discussed, taking into account the buffer layer calculated from Karman's three-layer model. A correlation was proposed for the obtained minimum film thickness in terms of the interfacial shear stress and the Reynolds number of the liquid. This correlation expressed the minimum film thickness obtained from the experiment to within 5%.

Acknowledgements

The authors wish to express their sincere thanks to Professors Takashi Hibiki of Kyoto University and Shu Takagi of the University of Tokyo for their advice and helpful discussions throughout this study. Part of this work was performed under the Grant-in-Aid for Scientific Research from Japan Society for the Promotion of Science (No. 16760653).

References

Azzopardi, B.J., 1986. Disturbance wave frequencies, velocities and spacing in vertical annular two-phase flow. Nucl. Eng. Des. 92, 121–133.

Clark, W.W., Hills, J.H., Azzopardi, B.J., 1999. Spatial film thickness measurements in falling films in a concurrent air flow using a novel adaptation of the light absorption technique. Proc. Two-Phase Flow Model. Exp. 1999, 1440–1453.

Dukler, A.E., Bergelin, O.P., 1952. Characteristics of flow in falling liquid film. Proc. Chem. Eng. Progr. Symp. Ser., 557–563.

Elsäßer, A., Samenfink, W., Ebner, J., Dullenkopf, K., Wittig, S., 1998. Effect of variable liquid properties on the flow structure within shear-driven wall films. Proc. Ninth Int. Symp. Appl. Laser Tech. Fluid Mech. 1–3, 1–10.

Fukano, T., Mori, S., Akamatsu, S., Baba, A., 2002. Relation between temperature fluctuation of a heating surface and generation of drypatch caused by a cylindrical spacer in a vertical boiling two-phase upward flow in a narrow annular channel. Nucl. Eng. Des. 217, 81–90.

Fukano, T., Mori, S., Nakagawa, T., 2003. Fluctuation characteristics of heating surface temperature near an obstacle in transient boiling two-phase flow in a vertical annular channel. Nucl. Eng. Des. 219, 47–60.

Hall-Taylor, N.S., Nedderman, R.M., 1968. The coalescence of disturbance waves in annular flow. Chem. Eng. Sci. 23, 551–564.

Hewitt, G.F., Nicholls, B., 1969. Film thickness measurement in annular two-phase flow using a fluorescence spectrometer technique, Part II: Studies of the shape of the disturbance waves. UKAEA Report, AERE-R4506.

Hewitt, G.F., Hall-Taylor, N.S., 1970. Annular Two-Phase Flow. Pergamon Press, Oxford.

Hewitt, G.F. et al., 1985. Experimental and modeling studies of annular flow in the region between flow reversal and the pressure drop minimum. PCH Physico-Chem. Hydrodyn. 6–1/2, 69–86.

Mori, K., Matsumoto, T., Uematsu, H., 1998. Time-spatial interfacial structures and flow characteristics in falling liquid film. In: Proceedings of the Third International Conference on Multiphase Flow, CD-ROM, #514.

Nasr-Esfahany, M., Kawaji, M., 1996. Turbulence structure under a typical shear induced wave at a liquid/gas interface. Proc. AIChE Symp. Ser., 203–210.

Ohba, K., Nakamura, K., Naimi, F., 1995. A new kind of interfacial wave on liquid film in vertically upward air–water two-phase annular flow. In: Proceedings of the Second International Conference on Multiphase Flow'95-Kyoto (ICMF'95), IP1, pp. 27–33.

Poltalski, S., Clegg, A.J., 1972. An experimental study of wave inception on falling liquid film. Chem. Eng. Sci. 27, 1257–1265.

Sekoguchi, K., Ueno, T., Tanaka, O., 1985. Flow characteristics of air–water annular flow (2nd report: correlation for flow parameter). Trans. Jpn. Soc. Mech. Eng. 51–466 (B), 1798–1806.

Sekoguchi, K., Mori, K., 1997. New developments of experimental study of interfacial structure in gas–liquid two-phase flow. Exp. Heat Transfer, Fluid Mech. Thermodyn. 2, 1177–1188.

Serizawa, A., Nagane, K., Ebisu, T., Kamei T., Kawara, Z., 1994. Dynamic measurement of liquid film thickness in satisfied flow by using ultrasonic echo technique. In: Proceedings of the Fourth International Topical Meeting on Nuclear Thermal-Hydraulics, Operations and Safety, pp. 42-C-1–42-C-5.

Serizawa, A., Kamei, T., Kataoka, I., Kawara, Z., Ebisu, T., Torikoshi, K., 1995. Measurement of dynamic behavior of a liquid film with liquid droplets in a horizontal channel. In: Proceedings of the Second International Conference on Multiphase Flow, vol. 6, pp. 27–34.

Takamasa, T., Hazuku, T., 2000. Measuring interfacial waves on film flowing down a vertical plate in the entry region using laser focus displacement meters. Int. J. Heat Mass Transfer 43, 2807–2819.

Takamasa, T., Kobayashi, K., 2000. Measuring interfacial waves on film flowing down tube inner wall using laser focus displacement meter. Int. J. Multiphase Flow 26, 1493–1507.

Ueda, T., Nose, S., 1973. Liquid film in annular two-phase flow (2nd report: vertical two-phase upward flow). Trans. Jpn. Soc. Mech. Eng., 2853–2862.